**Laboratoire de la construction métallique (ICOM)**
INSTITUT DE STRUCTURES
FACULTÉ ENVIRONNEMENT NATUREL, ARCHITECTURAL ET CONSTRUIT
ÉCOLE POLYTECHNIQUE FÉDÉRALE DE LAUSANNE

Rapport de mandat N° IC 704-2

# ANALYSIS OF STRESS CONCENTRATION AT LONGITUDINAL ATTACHMENT

Mandat de prestation
SBB, Berne

December 2005

FACULTE ENVIRONNEMENT NATUREL, ARCHITECTURAL ET CONSTRUIT ENAC
INSTITUT DE STRUCTURES IS
**LABORATOIRE DE LA CONSTRUCTION METALLIQUE ICOM**

ÉCOLE POLYTECHNIQUE
FÉDÉRALE DE LAUSANNE

EPFL ICOM
Bât. GC B3
CH-1015 Lausanne

Téléphone : + 4121 693 24 25
Fax : + 4121 693 28 68
E-mail : icom@epfl.ch
Site web : icomwww.epfl.ch /

**V/réf :** M. T. Lang, SBB

Lausanne, le 15 Décembre 2005

**N/réf :** AN/LB

Rapport IC **704-2**

# Analysis of stress concentration at longitudinal attachment

| | |
|---|---|
| **Mandant:** | Thomas P. Lang<br>Schweizerische Bundesbahnen SBB<br>Infrastruktur, Ingenieurbau<br>*Schanzenstrasse 5*<br>3000 BERNE 65 |
| **Définition du mandat:** | Influence de la forme d'une attache longitudinale sur la concentration de contraintes (SCF) et le facteur d'intensité de contrainte (SIF). Le rapport sera en anglais. |
| **Date du mandat:** | Vertrag NR 2004-0101, 13.2.2004<br>Nachtrag NR 1, 28.10.2004 |
| **Chef de projet :** | NUSSBAUMER Alain |
| **Collaborateur:** | BORGES Luis |
| **Auteurs du rapport:** | BORGES Luis, NUSSBAUMER Alain. |

Chef de projet

Dr. Alain Nussbaumer

Directeur de l'ICOM

Prof. Manfred A. Hirt

Ce rapport contient 32 pages

# TABLE OF CONTENTS

# 1 INTRODUCTION

Following ICOM's participation in the redaction of a new recommendation for the evaluation of existing railway-bridges, in collaboration with the SBB/CFF, new questions have been raised. Among those, the influence of a welded longitudinal attachment ends shape on its fatigue behaviour was of particular interest. Indeed, this detail has low fatigue strength (as low as detail category 56 according to SIA 263 [SIA 263]) and the possible shape improvements that are given in the code are costly to fabricate. Therefore, the pilot study presented in this report was initiated with the objective to better understand the influence of the attachment shape on the stress concentration and fatigue life of the detail. In order to achieve this objective, the following steps were carried out:

- Literature review on study of existing SCF solutions (2000-2003);
- Boundary Elements Modelling (BEM) of reference cases;
- Study of the influence of the attachment angle, shape, length on the SCF;
- Study of the influence of the attachment angle, shape, length on the SIF at various depths.

The scope of this study is limited to longitudinal attachment welded onto a plate (that is perpendicular and not to the edge of the plate), under tensile stress field.

During the course of this pilot study a progress report (ICOM 704-1) was issued. The current report recapitulates the whole and thus supersedes the progress report.

## 1.1 EXISTING SCF SOLUTIONS

For longitudinal attachments axially loaded, the following classical solutions exist in literature:

- Castiglioni [Castiglioni 1989] , [Castiglioni et al. 1992];
- Hobbacher [Hobbacher 1993], [Hobbacher 2003];

These solutions are based upon FEM analysis and do not account for different attachment shape (such as different angles or round details). A short bibliography list on longitudinal attachment fatigue behaviour publications can be found in annex (7.1).

## 1.2 METHODS FOR FATIGUE ANALYSIS OF WELDED STRUCTURES

In order to study the stress concentration factor, the following methods for stress determination at weld toe do exist [Radaj 1995] [Xiao et al. 2004] [Poutiainen et al. 2004.1]:

1. Structural hot-spot stress;
2. 1-mm stress;
3. Local stress at notch using Linear Elastic Fracture Mechanics (LEFM);
4. Dong method;
5. Through thickness at the weld toe (TTWT),
6. Hobbacher local stress method.

In this study, the first three methods are used and compared. These methods are now summarized.

### 1.2.1 Hot-spot stress

Structural hot spot surface stress, $\sigma_{hs}$, or geometric stress, includes all stress raising effects of a structural detail excluding all stress concentrations due to the local weld profile itself. The stress concentration factor (SCF) is the ratio between the hot spot stress, $\sigma_{hs}$, and the nominal stress, $\sigma_{nom}$ (away from stress rising singularity).

$$SCF = \frac{\sigma_{hs}}{\sigma_{nom}} \tag{1.1}$$

According to IIW - Fatigue Recommendations (XIII-1965-03/XV-1127-03 [Hobbacher 2003], (XIII-1819-00 [Niemi 2000]), it can be evaluated using FEM and taking the stress values at different distances from the weld toe (called reference points). When a fine mesh is used, the following three evaluations can be made:

- Type « a » hot spots:
  - Linear Extrapolation with 2 reference points at distances related to the base plate thickness *t* (0.4*t* and 1.0*t* from weld toe):

$$\sigma_{hs} = 1.67 \cdot \sigma_{0.4\,t} - 0.67 \cdot \sigma_{1.0\,t} \tag{1.2}$$

  - Quadratic Extrapolation with 3 reference points (at 0.4*t* and 0.9*t* and 1.4*t* from weld toe):

$$\sigma_{hs} = 2.52 \cdot \sigma_{0.4\,t} - 2.24 \cdot \sigma_{0.9\,t} + 0.72 \cdot \sigma_{1.4\,t} \tag{1.3}$$

- Type « b » hot spots:
  - Quadratic Extrapolation with 3 reference points at absolute coordinates: 4mm, 8mm and 12mm

$$\sigma_{hs} = 3 \cdot \sigma_{4mm} - 3 \cdot \sigma_{8mm} + \sigma_{12mm} \tag{1.4}$$

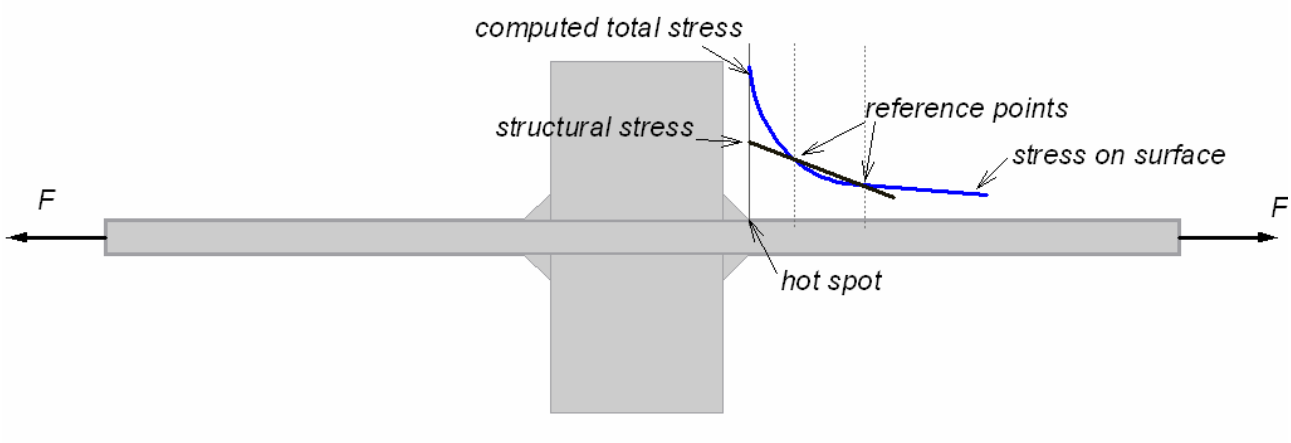


***Fig. 1.1:*** *Extrapolation to determine hot-spot stress at weld toe*

### 1.2.2 Stress distribution in weld toe region: through thickness

A new method for evaluating the geometric or structural stress in welded connections was proposed by Xiao and Yamada [Xiao et al. 2004]. This method is based on the computed stress value 1-mm below the surface in the direction of the expected crack path. It assumes the total stress distribution along the crack path to be the sum of the geometric stress caused by the structural geometry change and the highly non-linear local stress produced by the weld itself.

This method considers that the stress concentration at weld toe is composed of two parts: the local peak stress due to weld profile and the geometric stress or hot-spot stress due to structural geometry change (longitudinal attachment) as described by:

$$K_t = K_w \cdot K_s \tag{1.5}$$

Where $K_t$ is the whole stress concentration at weld toe; $K_w$, the stress concentration due to weld profile; and $K_s$, the structural geometry change stress;

The whole stress of a small size cruciform joint as represented in Fig. 1.2 is thought to be equivalent to the local stress produced by the weld itself.

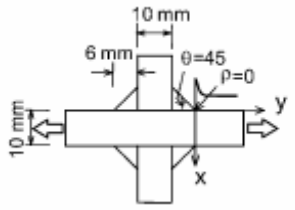


***Fig. 1.2:*** *Reference detail to assess local stress produced by weld profile* ***[Xiao et al. 2004]****.*

In order to derive the structural stress, Xiao proposes to calculate the total stress and the stress produced by the local weld profile (obtained with a cruciform joint with the same weld toe geometry selected as a reference detail to express the local effect, Fig. 1.2). The structural stress is then approximated by their ratio. At a depth of 1 mm, the following relationship can be written:

$$K_t(1\text{mm}) = K_s(1\text{mm}) \cdot K_w(1\text{mm}) \tag{1.6}$$

Once the stress concentration due to the weld profile, $K_w(1\text{mm})$, is approximately 1 at this depth, then $K_s(1\text{mm}) \approx K_t(1\text{mm})$.

This procedure was followed in the case of the longitudinal attachment.

According to Xiao [Xiao et al. 2004], a good correlation of crack propagation life can be established between studied detail and reference detail by using the geometric stress at a certain point along the crack path line. The following formula can be used to estimate the fatigue life of a detail based upon its structural stress at 1mm in depth in the weld toe:

$$N_p = \frac{1}{\left[K_s(1\text{mm})\right]^m} \cdot N_{pr} \tag{1.7}$$

$N_p$ : Life to propagate a crack from an initial size of 0.1mm to a size of 10 mm;

$N_{pr}$ : Life to propagate a crack from an initial size of 0.1mm to a size of 10 mm for the reference detail;

$K_s$(1mm) : Structural stress at 1mm in depth;

m : Material related parameter (Paris Crack Growth Law);

An example of BEM model to calculate the stress gradient in depth is shown in Fig. 1.3, with the line along which the stress is taken.

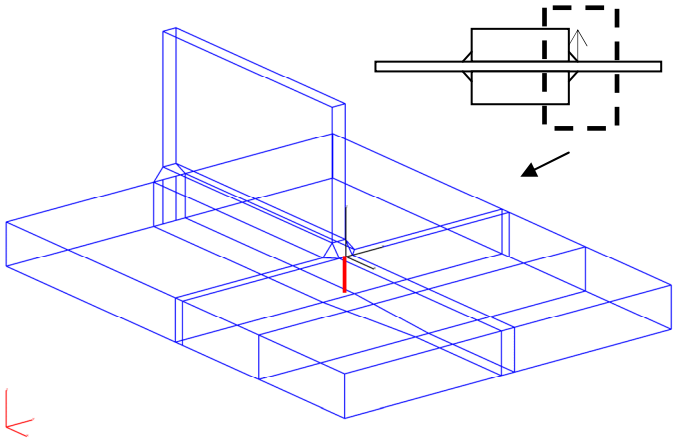

***Fig. 1.3:*** *BEM model of the longitudinal attachment, with line for stress distribution evaluation (corresponding to crack path)*

Note that the exact depth found was equal 1.3mm, though, due to the flat stress gradient of geometric stress the stress at 1 mm in crack path results in a good correlation of fatigue propagation life.

Since the studied detail and the reference detail may have different crack length values the correlation might not be performed through the whole range of crack propagation. However, since most of the fatigue life is consumed when the crack is still small, the influence of the range on fatigue life is not so significant.

### 1.2.3 Linear Elastic Fracture Mechanics (LEFM)

In this method, one searches to describe the stress state in the vicinity of the tip of a crack. It has been shown by Irwin [Broek 1986], that the stress state very close to the tip of a crack in a ductile material, as well as in a brittle one, can be uniquely described with a parameter. This parameter is refered to as the stress intensity factor (SIF) or K. Further, it has been shown that the range of this parameter, ΔK, can be used to characterise fatigue crack propagation. In general, ΔK can be described by the following expression:

$$\Delta K = M_k \cdot Y \cdot \Delta\sigma \cdot \sqrt{\pi \cdot a} \tag{1.8}$$

$a$ : crack depth;

$\Delta\sigma$ : stress range;

$Y$ : correction factor for different 1-dimensional or 2-dimensional crack shapes and boundary conditions;

$M_k$ : magnification factor for non-uniform applied stress distribution;

$Y$ and $M_k$ can be found in literature. In the case of longitudinal attachments we have carried out a review. The following solutions do exist for $M_k$:

- Hobbacher
- Castiglioni

Values for $\Delta K$ can also be extracted from FEM or BEM models using various techniques. In Beasy, the stress intensity factors (SIF) are computed using crack opening displacement method [BEASY 2003].

Using the Paris law, the applied stress intensity factor range can be related to the rate of crack growth as follows:

$$\frac{da}{dN} = D \cdot \Delta K^n \tag{1.9}$$

D, n : constant and exponent of Paris law.

$\frac{da}{dN}$ : crack propagation rate.

Integrating Paris law between an initial and final crack size permits the calculation of the fatigue life of a structural detail.

Some software packages, such as Beasy [BEASY 2003], can also carry out automatic crack growth calculations, with remeshing at each crack size step.

# 2 MODELING

A Boundary Element Method (BEM) commercial package, BEASY [BEASY 2003], was used to model the studied cases.

## 2.1 LOADING

All the models were calculated for a unitary uniform tensile stress field applied longitudinally at the extremity (Fig. 2.1).

## 2.2 SYMMETRY CONSIDERATIONS / BOUNDARY CONDITIONS

A ¼ model of the specimen was modelled. Two symmetry planes were then considered with the respective boundary conditions as illustrated in Fig. 2.1.

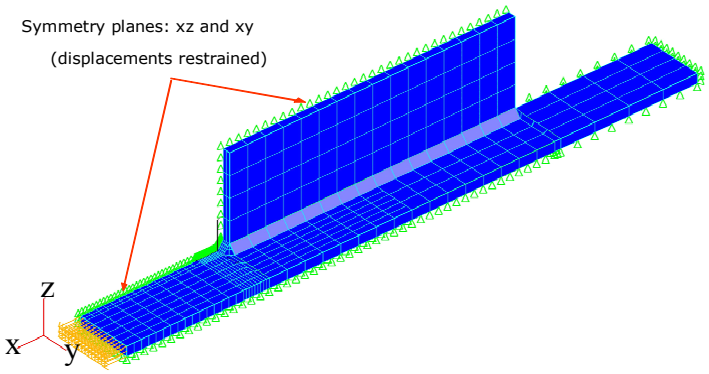


***Fig. 2.1:*** *Symmetry planes and boundary conditions – Model type I.*

This model was preferred in a first step (calculation of hot-spot stresses and stress intensity factors) because it could allow for unsymmetrical load conditions. In this pilot study, this was not explored.

In a second step, in order to apply the 1 mm stress method (see paragraph 4.5), all calculated cases were re-modelled following a different strategy (see Fig. 2.2) so that the stress in depth in the weld toe could be calculated with a good accuracy. This second modelling revealed to be much faster to compute because of the reduced number of boundary elements between modelling zones. In this model the global equilibrium was provided by means of flexible spring supports applied at the top face of the longitudinal attachment.

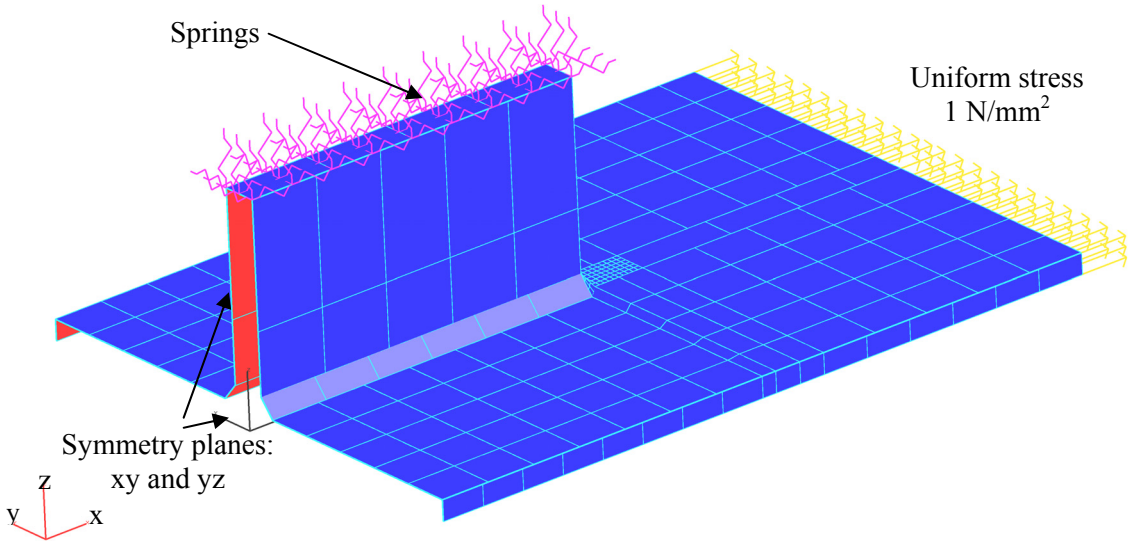


***Fig. 2.2:*** *Symmetry planes and boundary conditions – Model type II.*

## 2.3 STRESS AT REFERENCE POINTS FOR HOT SPOT METHOD

The boundary element mesh used was manually defined in front of the weld toe in order to ensure a good precision of results a refinement (Fig. 2.3) was established in the vicinity, where nonlinear stress becomes steeper.

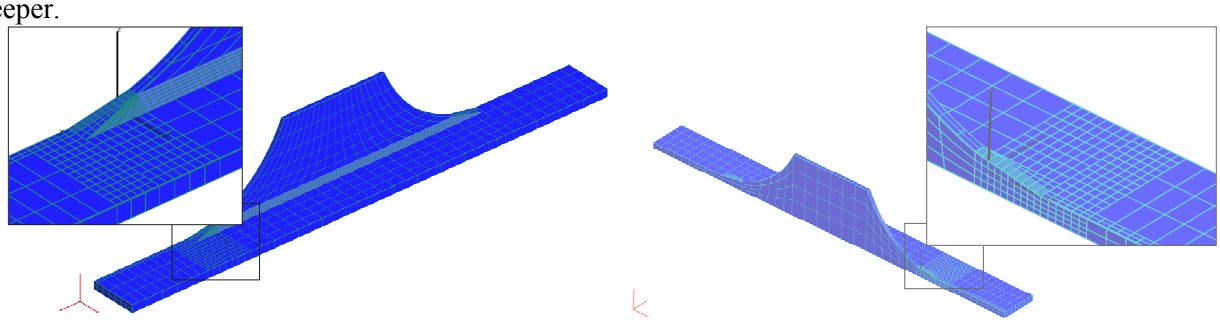

***Fig. 2.3:*** *Example of model mesh detail (Case_20_12_400_S(150)_W(150)).*

The stresses at reference points were calculated by interpolating stresses in neighbour mesh points, according to the scheme shown in Fig. 2.4. Once these known, extrapolation according to the different equations given in 1.2.1 can be made.

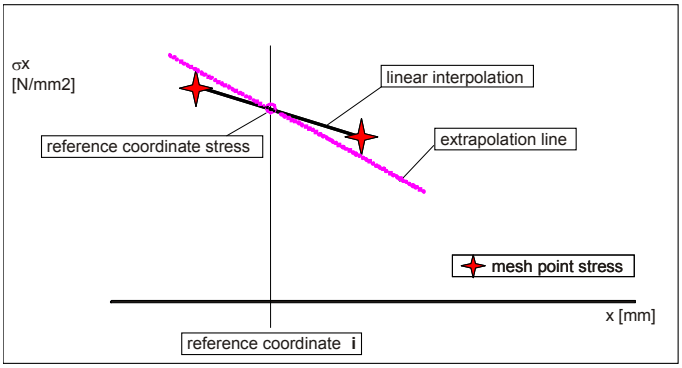


***Fig. 2.4:*** *Interpolation to get stress at reference points.*

## 2.4 CRACK MODELING

Cracks were modelled using BEASY *fracture mechanics* wizard. A semi-circular initial crack with 21 elements was chosen (a/c=1) (Fig. 2.5) and an initial crack depth of 0.15 mm was prescribed for all cases in order to calculate stress intensity factors (model type I).

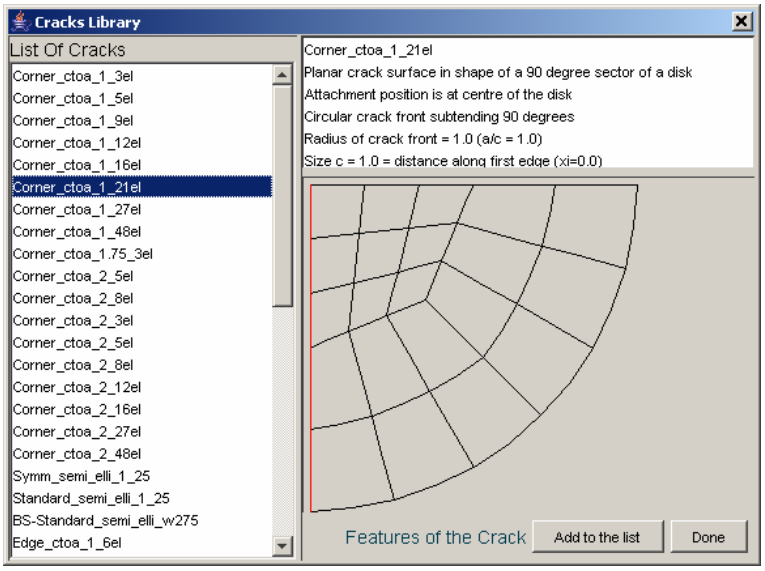


***Fig. 2.5:*** *Initial crack mesh used to calculate SIF values.*

## 2.5 CRACK PROPAGATION

Crack propagation was carried-out using BEASY *fracture mechanics wizard*. The crack shape does not remain constant, it is adapting incrementally according to the different SIF values along the crack front model, thus simulating more realistically the growth of a 2-dimensional crack. The example presented in paragraph 4.4 was calculated using model type II, which proved to be more efficient, with a semicircular initial crack of 0.15mm meshed with 24 elements.

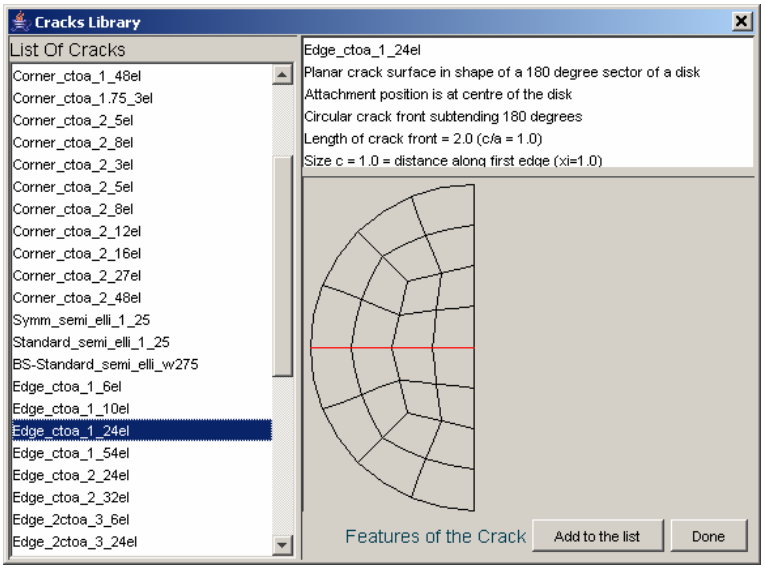


***Fig. 2.6:*** *Initial crack mesh used to perform crack propagation.*

# 3 PARAMETRIC STUDY

The parametric study was related to the following Eurocode 3 [prEN 1993-1-9:2003] detail categories (Fig. 3.1).

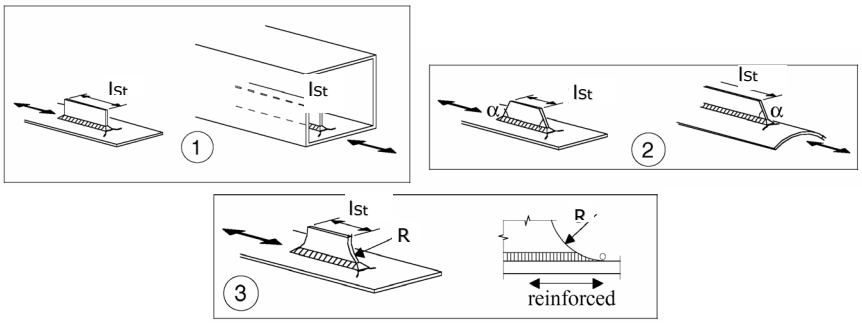


***Fig. 3.1:*** *Eurocode referenced details (table 8.4) [prEN 1993-1-9:2003]*

The studied cases cover longitudinal attachment plates with rectangular, trapezoidal and round shapes- Tab. 3.1. Four models are shown in Fig. 3.2.

The fatigue category classification (Tab. 3.1) was taken from EC3 part 1.9 Table 8.4 [prEN 1993-1-9:2003].

The weld profile angle was also considered a parameter as shown in Tab. 3.1. It is important to state that in table 8.4 from part 1-9 there's no reference to weld angles. One can assume it is assumed being around 45°.

From now on the different cases are referred to by the following code: **Case**_$t_{Bpl}$_$t_{st}$_$l_{st}$_**S**$\alpha$**(***R***)_W***angle*(*radius*)** where $t_{Bpl}$ stands for the thickness of the base plate, $t_{st}$ thickness of the stiffener, S is followed by the stiffener angle or radius (in brackets) and, when necessary, W followed by the welding angle or radius(in brackets) whenever it is different from 45°.

***Tab. 3.1:*** *Parametric study*

| Case | | Stiffener | | | | | Base Plate | | | Weld |
|---|---|---|---|---|---|---|---|---|---|---|
| | CAT | α | R | $t_{St}$ | $l_{St}$ | $h_{St}$ | $t_{Bpl}$ | $l_{Bpl}$ | $b_{Bpl}$ | Angle (radius) |
| | | [°] | [mm] | [mm] | [mm] | [mm] | [mm] | [mm] | [mm] | ° (mm) |
| **Case_20_12_80_S90°** | **71** | **90** | **-** | **12** | **80** | **100** | **20** | **800** | **150** | **45** |
| **Case_20_20_400_S90°** | **56** | **90** | **-** | **20** | **400** | **100** | **20** | **800** | **150** | **45** |
| **Case_20_12_400_S90°** | **56** | **90** | **-** | **12** | **400** | **100** | **20** | **800** | **150** | **45** |
| **Case_40_12_400_S90°** | **56** | **90** | **-** | **12** | **400** | **100** | **40** | **800** | **150** | **45** |
| **Case_30_12_400_S90°** | **56** | **90** | **-** | **12** | **400** | **100** | **30** | **800** | **150** | **45** |
| **Case_60_12_400_S90°** | **56** | **90** | **-** | **12** | **400** | **100** | **60** | **800** | **150** | **45** |
| **Case_100_12_400_S90°** | **56** | **90** | **-** | **12** | **400** | **100** | **100** | **800** | **150** | **45** |
| Case_20_12_400_S90°_W45x | | 90 | - | 12 | 400 | 100 | 20 | 800 | 150 | $45^{x}$ |
| Case_10_6_300_S90° | | 90 | - | 6 | 300 | 60 | 10 | 600 | 100 | 45 |
| **Case_20_12_400_S45°** | **71*** | **45** | **-** | **12** | **400** | **100** | **20** | **800** | **150** | **45** |
| Case_20_12_400_S45°_W(150) | **71** | 45 | - | 12 | 400 | 100 | 20 | 800 | 150 | (150) |
| **Case_20_12_400_S30°_W30°** | **71** | **30** | **-** | **12** | **400** | **100** | **20** | **800** | **150** | **30** |
| **Case_20_12_400_S30°** | **71** | **30** | **-** | **12** | **400** | **100** | **20** | **800** | **150** | **45** |
| **Case_20_12_400_S(150)_W(150)** | **80** | **-** | **150** | **12** | **400** | **100** | **20** | **800** | **150** | **(150)** |

Note that the weld toe radius was assumed to be zero, except for cases with weld ground and circular shape end.

Due to the time consuming calculation process, cases in bold were selected from Tab. 3.1 in order to be run in a first stage. Other cases will be considered in future work.

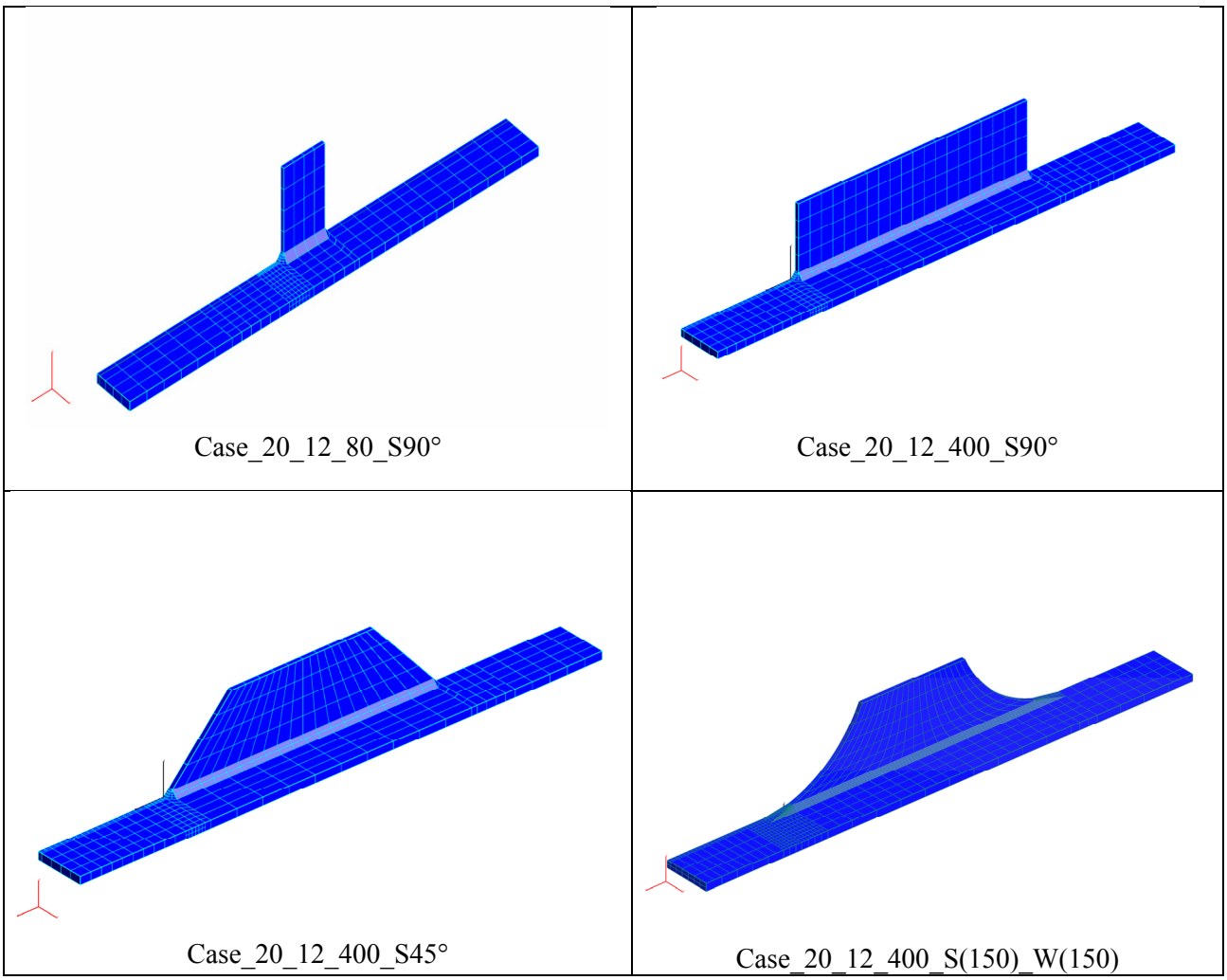


***Fig. 3.2:*** *Different BEASY models (Type I).*

# 4 RESULTS AND DISCUSSION

## 4.1 STRESS PATH

As expected, longitudinal stresses rise towards infinity near the weld toe of the longitudinal attachment. Fig. 4.1 summarizes the stress paths for the different cases studied (details for each case can be found in annex).

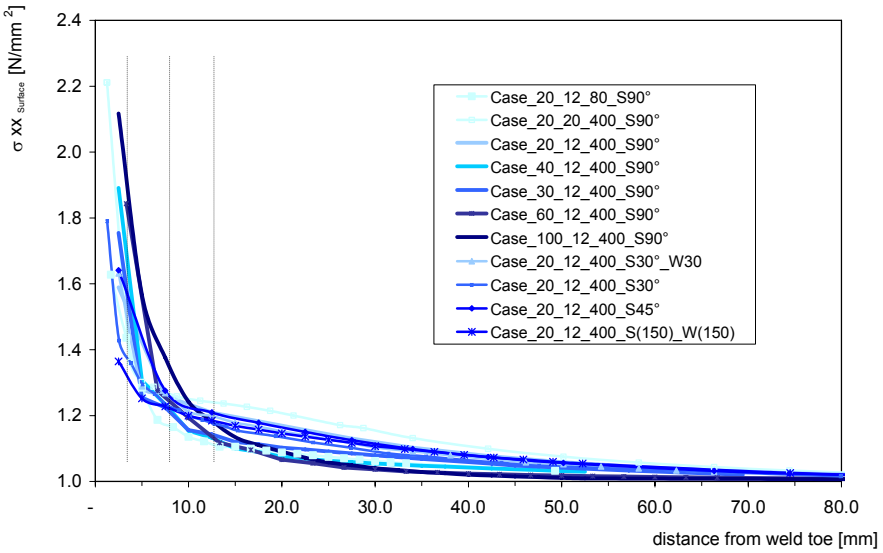


***Fig. 4.1:*** *Longitudinal stress evolution on the surface towards the weld toe.*

## 4.2 HOT-SPOT STRESSES

The hot spot stresses, $\sigma_{hs}$, were calculated following the procedure described in section 1.2.1. Fig. 4.2 shows an example of the stress field and extrapolation made.

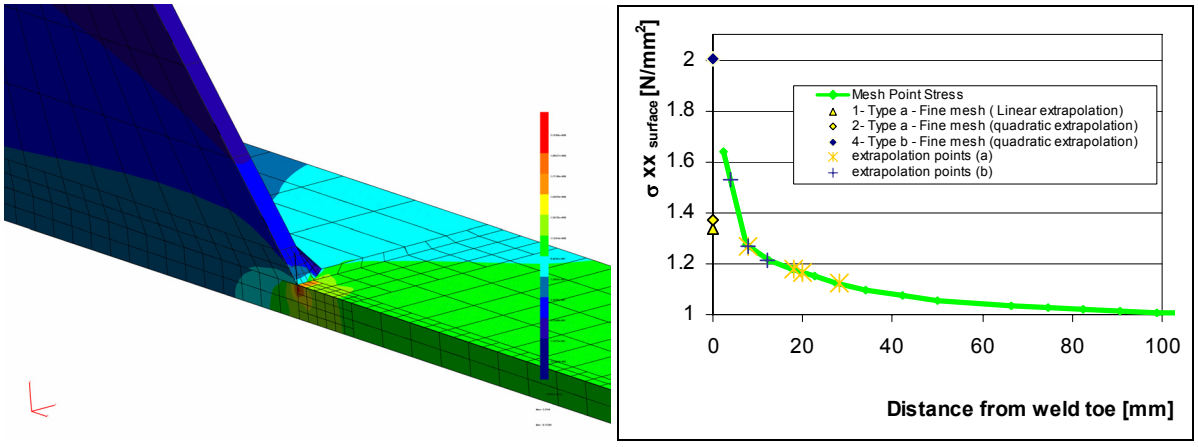


***Fig. 4.2:*** *Hot-spot stress calculation (Case_20_12_400_S45°)*

The results obtained are presented in Tab. 4.1 and expressed using the stress concentration factor (SCF) values rather than hotspot stresses. Note that since an unitary nominal stress value was used in the models, both are identical.

***Tab. 4.1:*** *SCF results*

| Case | SCF | | |
|---|---|---|---|
| | type a | | type b |
| | linear | quadratic | quadratic |
| Case_20_12_80_S90° | 1.22 | 1.26 | 1.74 |
| Case_20_20_400_S90° | 1.33 | 1.33 | 1.49 |
| Case_20_12_400_S90° | 1.31 | 1.33 | 1.92 |
| Case_40_12_400_S90° | 1.19 | 1.24 | 2.10 |
| Case_30_12_400_S90° | 1.08 | 1.17 | 1.88 |
| Case_60_12_400_S90° | 1.08 | 1.10 | 2.61 |
| Case_100_12_400_S90° | 1.03 | 1.04 | 2.51 |
| Case_20_12_400_S45° | 1.34 | 1.37 | 2.00 |
| Case_20_12_400_S30°_W30° | 1.33 | 1.36 | 1.71 |
| Case_20_12_400_S30° | 1.29 | 1.33 | 1.55 |
| Case_20_12_400_S(150)_W(150) | 1.27 | 1.30 | 1.41 |

After ranking the cases according to their SCF value (Tab. 4.2 and Tab. 4.3) and comparing to the Fatigue Categories proposed by Eurocode 3, part 1-9 [prEN 1993-1-9:2003] we can notice that there is no correlation for *type a* extrapolation methods. A better correlation is achieved by SCF type b although there are contradictions for *Case_20_20_400_S90°* and *Case_20_12_400_S45°*.

***Tab. 4.2:*** *Case ranking (SCF a)*

| | Case | Fat. Cat. | SCF a lin. | SCF a qua. |
|---|---|---|---|---|
| | Case_100_12_400_S90° | 56 | 1.03 | 1.04 |
| | Case_60_12_400_S90° | 56 | 1.08 | 1.10 |
| | Case_30_12_400_S90° | 56 | 1.08 | 1.17 |
| | Case_40_12_400_S90° | 56 | 1.19 | 1.24 |
| | Case_20_12_80_S90° | 71 | 1.22 | 1.26 |
| | Case_20_12_400_S(150)_W(150) | 80 | 1.27 | 1.30 |
| | Case_20_12_400_S30° | 71 | 1.29 | 1.33 |
| | Case_20_20_400_S90° | 56 | 1.33 | 1.33 |
| | Case_20_12_400_S90° | 56 | 1.31 | 1.33 |
| | Case_20_12_400_S30°_W30° | 71 | 1.33 | 1.36 |
| | Case_20_12_400_S45° | 71 | 1.34 | 1.37 |

***Tab. 4.3:*** *Case ranking (SCF b)*

| | Case | Fat. Cat. | SCF b |
|---|---|---|---|
|  | Case_20_12_400_S(150)_W(150) | **80** | 1.41 |
| | Case_20_20_400_S90° | **56** | 1.49 |
| | Case_20_12_400_S30° | **71** | 1.55 |
| | Case_20_12_400_S30°_W30° | **71** | 1.71 |
| | Case_20_12_80_S90° | **71** | 1.74 |
| | Case_30_12_400_S90° | **56** | 1.88 |
| | Case_20_12_400_S90° | **56** | 1.92 |
| | Case_20_12_400_S45° | **71** | 2.00 |
| | Case_40_12_400_S90° | **56** | 2.10 |
| | Case_100_12_400_S90° | **56** | 2.51 |
| | Case_60_12_400_S90° | **56** | 2.61 |

## 4.3 STRESS INTENSITY FACTORS

In order to take in consideration both surface geometric stress and stress gradient in depth, a crack was introduced at the weld toe. Stress intensity factors (K or SIF) at various crack depths were computed. Stress intensity factors (SIF) values for the various cases studied are presented in Tab. 4.4. They were obtained considering an initial semi-circular crack of $a_0$= 0.15 mm, letting it become elliptical as the crack progresses.

***Tab. 4.4:*** *Case ranking (SIF)*

| | Case | CAT. | SIF [Nmm$^{-3/2}$] $a_0$=0.15 |
|---|---|---|---|
|  | Case_20_12_400_S(150)_W(150) | **80** | 0.75 |
| | Case_20_12_400_S30° | **71** | 1.11 |
| | Case_20_12_80_S90° | **71** | 1.56 |
| | Case_20_12_400_S30°_W30° | **71** | 1.67 |
| | Case_40_12_400_S90° | **56** | 1.81 |
| | Case_20_12_400_S90° | **56** | 1.83 |
| | Case_20_12_400_S45° | **71** | 1.84 |
| | Case_30_12_400_S90° | **56** | 1.87 |
| | Case_20_20_400_S90° | **56** | 1.88 |
| | Case_60_12_400_S90° | **56** | 2.07 |
| | Case_100_12_400_S90° | **56** | 2.13 |

The distribution looks logical but for cases *Case_20_12_400_S90°* and *Case_20_12_400_S45°*, the tendency seems to contradict the classification. That is to say that *Case_20_12_400_S45°* (the 45° attachment) seems to be not as favourable as it would be expected. This confirms the SCF, type b, results.

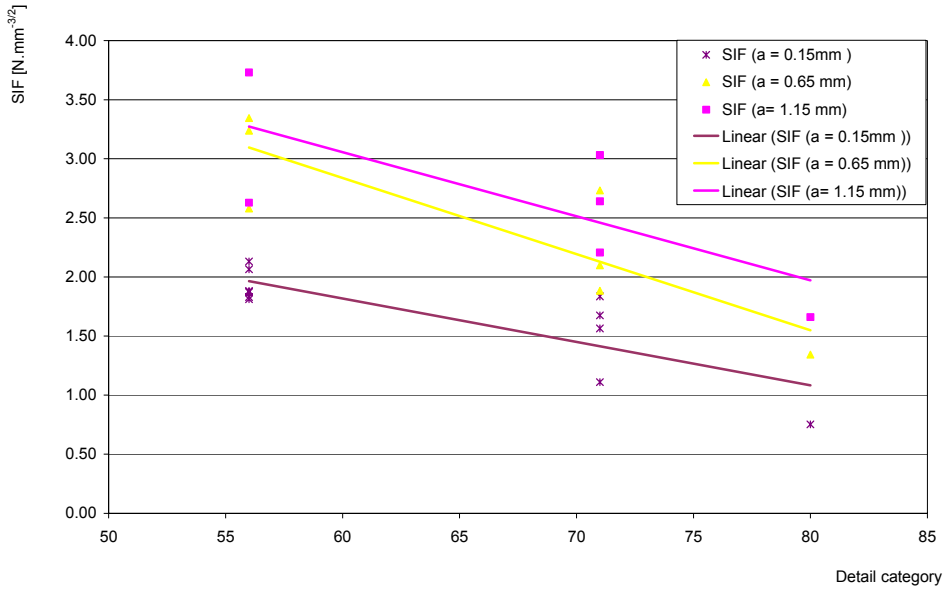


***Fig. 4.3:*** *Stress Intensity Factors and detail categories for different cases.*

From the analysis of SIF at 0.15mm crack depth (Tab. 4.4 and Fig. 4.4) we can notice that the results do not contradict the EC3 classification. Fig. 4.3 shows a tendency of decreasing SIF with increasing category but when looking at individual cases, one sees that the lowest SIF from cat 56 is close to the ~~heist~~ value from cat 71. Thus it's still not possible to unambiguously establish the category based upon the SIF at 0.15 mm or other depths.

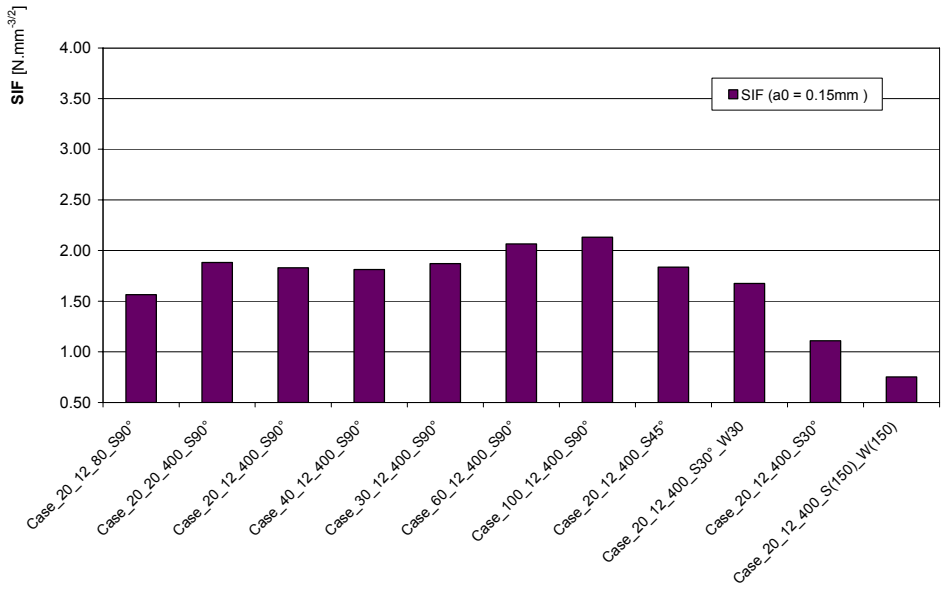


***Fig. 4.4:*** *Stress intensity factors at a 0.15mm crack depth comparison*

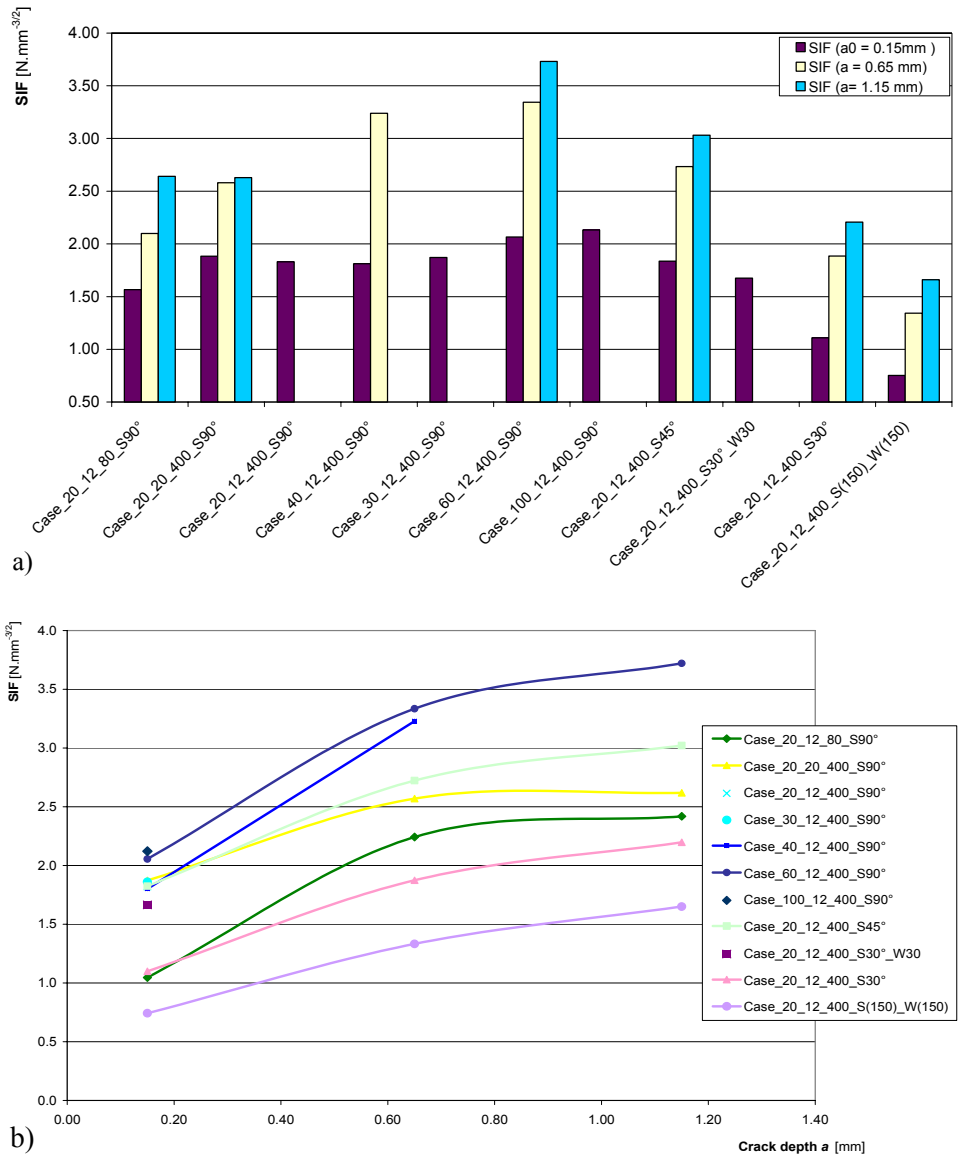


***Fig. 4.5:*** *Stress intensity factors at different crack depths: a) comparison with bars showing different cases b) SIF evolution with crack depth* a

In order to better understand crack propagation for the different cases, Fig. 4.5 presents the SIF evolution for different crack depths *a*. We can observe how some of the curves cross. The fatigue life of a detail depends on this evolution and not exclusively on the SIF at a given crack depth. However it's well known that early stages of the crack propagation consume most of the fatigue life of welded details.

## 4.4 CRACK PROPAGATION

In order to study the crack growth and be able to carry out a fatigue life analysis, incremental crack propagation was carried-out for *Case_20_20_400_S90°*. The crack propagation was calculated using BEASY Crack Propagation Wizard for model type II (Fig. 4.6). This calculation is time consuming. The example here below was calculated using 20 increments. A constant stress range, $\Delta\sigma$= 56 N/mm$^2$, was applied and the crack life was calculated using the Paris Law given in 1.2.3. The parameters of the law are taken as $D = 2 \cdot 10^{-13}\,(\text{mm/cycle}) \cdot (\text{Nmm}^{-3/2})$ and $n = 3$. These values are characteristic values for C-Mn steels [Hirt,

M.A. TGC 10]. The initial crack size used (0.150 mm) was chosen to represent imperfections depth generally present at weld toes (in the range 0.1 to 0.25 mm)

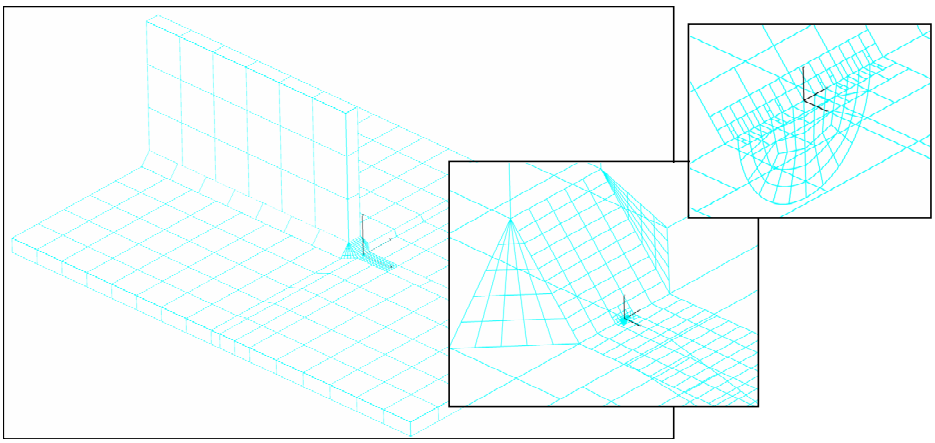

***Fig. 4.6:*** *Crack modelled in the weld toe (a=0.50mm)*

The results of the computation are shown in Fig. 4.7, in a graph with the number of cycles versus the crack size, in the width and depth direction. The crack at the end of the calculation is shown in figure 4.9. Note that the values of fatigue life can be compared since, both for S-N curve and crack propagation law parameters, characteristic values were used. One sees that there is a good correlation since the predicted fatigue life is about 2.2 Million cycles (for crack depths over 9 mm, the propagation is rapid and becomes unstable) for a stress range equal to the detail category.

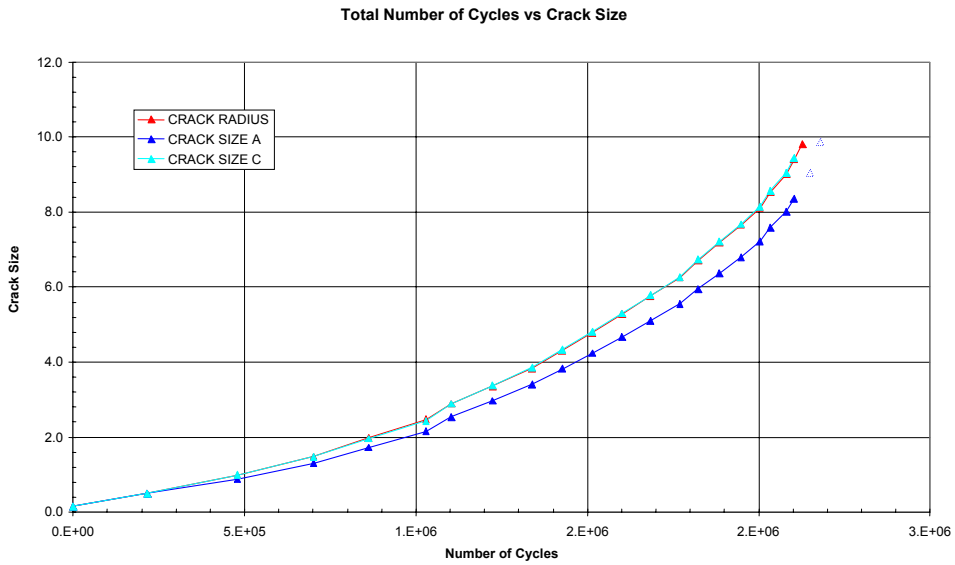


***Fig. 4.7:*** *Fatigue life for crack propagation from $a_i$=0.15mm to $a_f$≈ 9.0mm*

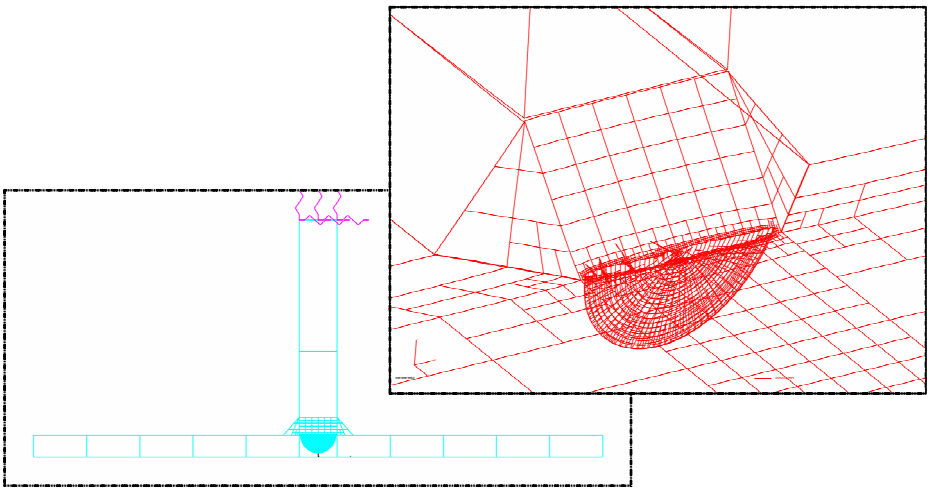

***Fig. 4.8:*** *Crack size and shape after 2.13E+06 cycles (20 increments)*

## 4.5 STRESS IN DEPTH

The stress distribution along the crack path direction was calculated (using models of type II). Twenty internal points were placed along the thickness in the weld toe in order to get accurate stress values in this highly nonlinear zone. These results allowed for the application of the recently proposed 1-mm method [Xiao et al. 2004] for evaluation of the geometric or structural stress in constructions. The longitudinal stress gradient in depth along the crack path was calculated for all the considered cases.

It should be pointed out that the stress at weld toe is theoretically infinite, and values obtained are only due to the finite size of the elements in the model.

The results obtained for the different cases are shown in Fig. 4.9. From this figure, it can be seen that stress in depth shows the same as stress on surface. Logically, the worse case (case with the highest $K_t$) is case 100_12_400_S90. Also, it can be seen that cases 20_12_400_S30_W30 and 20_12_400_S(150)_W(150), two cases with different shape but same plate thickness, present a different, more favourable, stress gradient in depth.

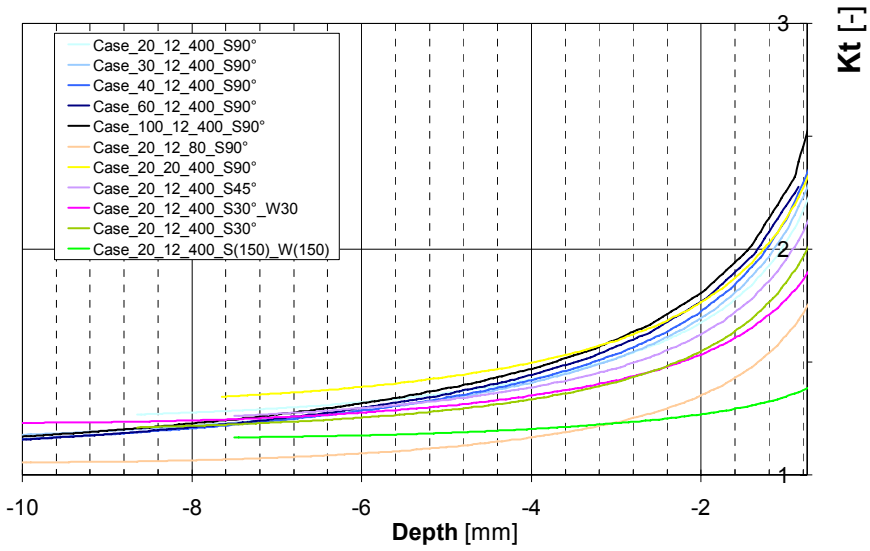


***Fig. 4.9:*** *Longitudinal Stress depth concentration along the crack path direction at the weld toe.*

Tab. 4.5 shows the ranking of cases according to their $K_t$ values at 1 mm in depth. Although a good match to EC3 categories is evident, it has to be noticed that once again, the value of $K_t$ for *Case_20_12_400_S45°* is much closer to values of cases belonging to fatigue category 56 than to the other "category 71" cases. This case should be studied more carefully in order to assess its fatigue behaviour and classification.

***Tab. 4.5:*** *$K_t$ results and case ranking.*

| Case | CAT. | Kt |
|---|---|---|
| Case_20_12_400_S(150)_W(150) | 80 | 1.35 |
| Case_20_12_80_S90° | 71 | 1.62 |
| Case_20_12_400_S30°_W30° | 71 | 1.78 |
| Case_20_12_400_S30° | 71 | 1.85 |
| Case_20_12_400_S45° | 71 | 1.95 |
| Case_20_12_400_S90° | 56 | 2.03 |
| Case_30_12_400_S90° | 56 | 2.08 |
| Case_40_12_400_S90° | 56 | 2.13 |
| Case_20_20_400_S90° | 56 | 2.13 |
| Case_60_12_400_S90° | 56 | 2.19 |
| Case_100_12_400_S90° | 56 | 2.26 |

### 4.5.1 Scale effect

From *Fig. 4.9*, one can isolate the cases where the only parameter that varies is the thickness in order to see its effect. This effect is clearly shown in *Fig. 4.10*. The thicker the base plate is, the higher stress concentration is obtained in depth in the weld toe. Although we should look at the EC3 classification with precaution, the 1-mm stress method results enhance the trust and confidence in the order these details appear regarding their fatigue strength. This will be further shown later using the structural stress in depth values $K_s$.

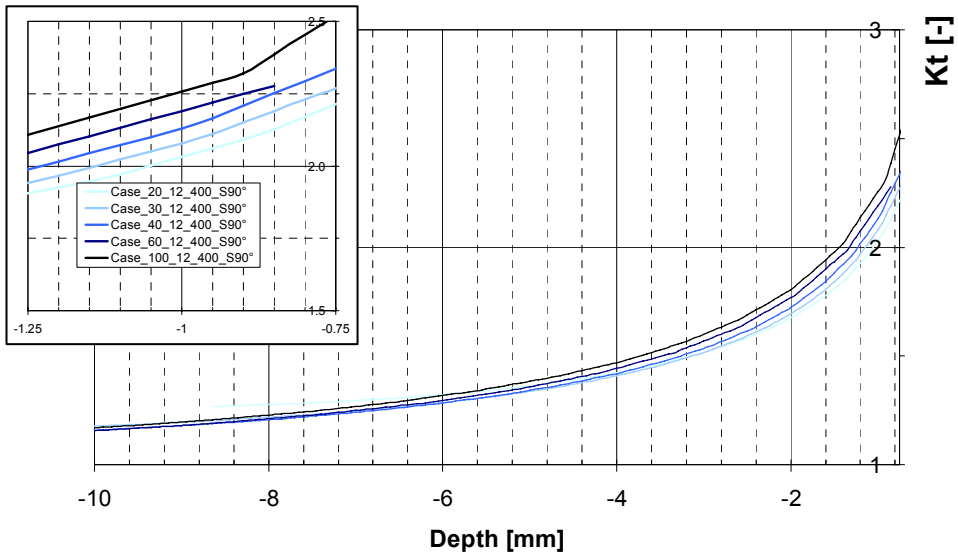


***Fig. 4.10:*** *Stress concentration gradient in depth for different thicknesses.*

### 4.5.2 Effect of Shape of Stiffener and Weld

The effect of shape is shown in Fig. 4.11. Compared to the effect of thickness, it is seen to be more significant. This explains that, for the longitudinal attachment, there is no thickness correction in the fatigue codes. In the fatigue test results database used to classify the details in the categories, the thickness effect is hidden within experimental error (variations in weld size, shape, testing rig, etc.). In this respect, it would be interesting to compare modelled details with real ones on SBB bridges, for example to get information about weld angle, weld size, range of thicknesses of the plates.

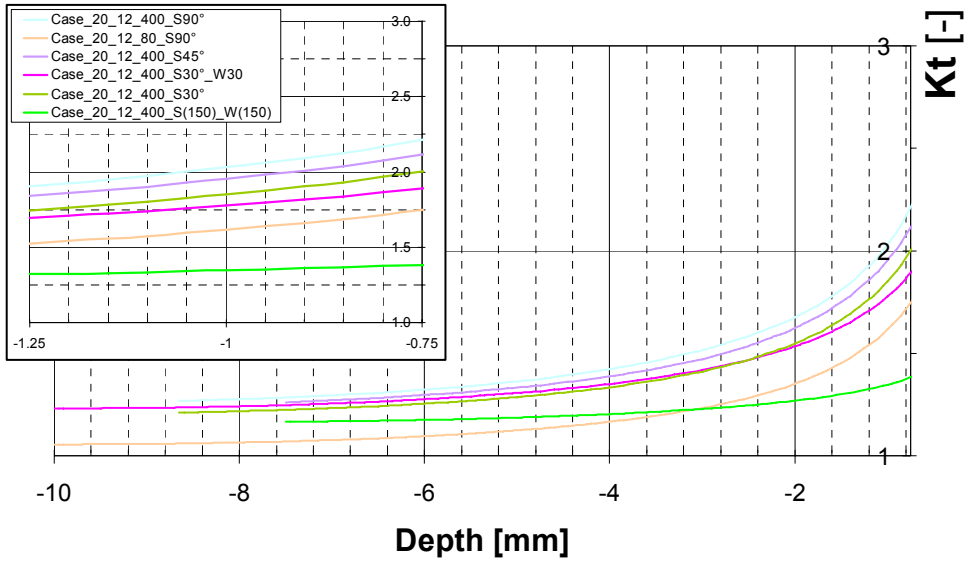


***Fig. 4.11:*** *Effect of detail shape over the stress gradient in depth.*

### 4.5.3 Structural Stress in depth

In order to determine the structural stress in depth, a reference detail must be chosen. We chose the same reference detail as used by Xiao [Xiao et al. 2004]. The stress in depth for the reference detail is shown in Fig. 4.12.

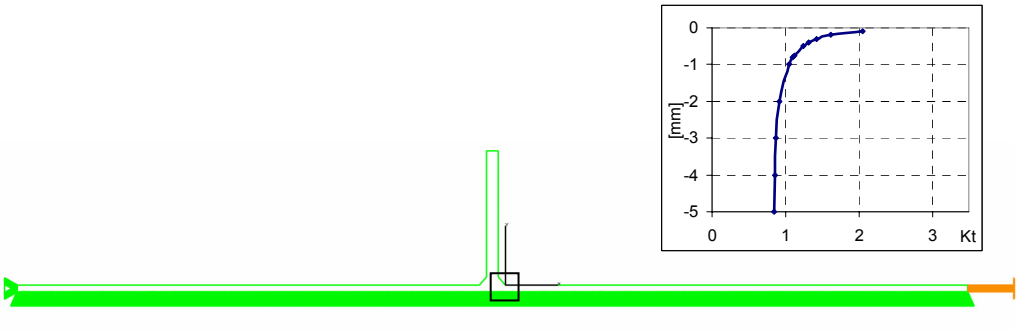


***Fig. 4.12:*** *Cruciform reference Joint (10 x 10, a=4.42mm θ=45°) [Xiao et al. 2004]*

Following the 1-mm method procedure [Xiao et al. 2004], the local stress concentration due to the weld profile can now be expressed; Dividing the total stress by the stress due to the weld profile (reference detail) (equation (1.5)) we obtain the structural stress. Structural stress gradients along the depth are shown in Fig.

4.13. As expected, the trend shown is in most cases linear. Again and as expected, the two cases with different shape, namely cases 20_12_400_S30_W30 and 20_12_400_S(150)_W(150), do not follow the general trend. Probably that another reference detail should ~~not~~ be chosen for these cases, but we do not know yet which one would be the most appropriate. Thus, for the time being, the $K_s$ values found using the same reference detail for all cases are used. The value of $K_s$ at 1 mm depth can now be used to compare different details, and also to compare the fatigue life of the details, as it is done in the next section.

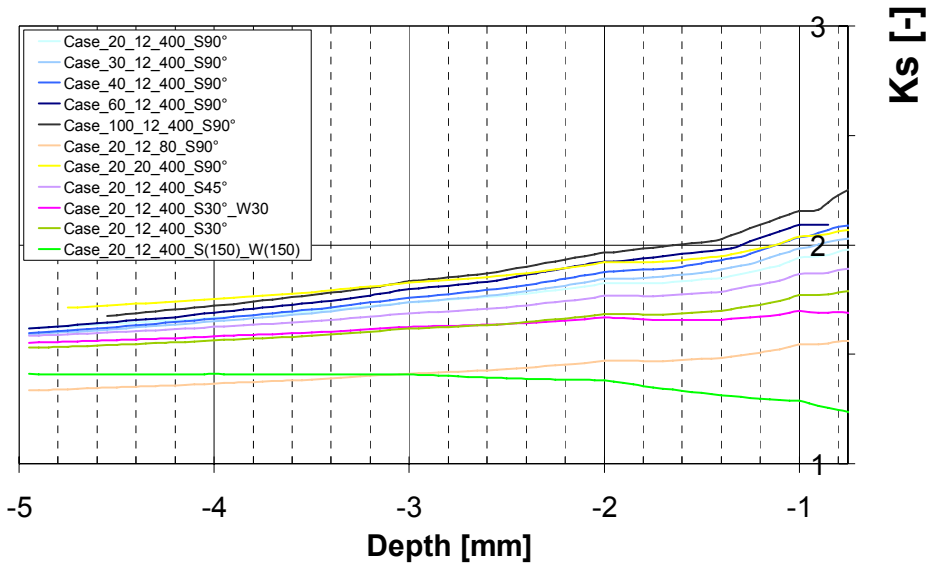


***Fig. 4.13:*** *Structural stress obtained along the crack path direction at the weld toe.*

### 4.5.4 Correlation of crack propagation life between object detail and reference detail

The values for the structural stress at a depth of 1 mm are summarized in Tab. 4.6, together with the detail categories. As can be seen, the classification is the same for both CAT and $K_s$. This does not change from what was seen in table 4.4 with SIF values. The characteristic value of the reference detail fatigue strength is, according to [Xiao et al. 2004], 102 MPa. Since this strength corresponds to 2 million cycles, one can compute the fatigue life for other stress range levels (S-N curve with slope m = 3), and also the fatigue life of other details using the following relationship:

$$N_p = \frac{N_{pr}}{K_s^m} \tag{4.1}$$

$N_p$ : propagation life for the detail under study;

$N_{pr}$ : propagation life for the reference detail, at the detail category $\Delta\sigma_C$ stress range;

$K_s$ : structural stress at 1 mm for the detail under study;

$m$ : slope of the S-N curve, assumed equal to 3.

The results of these computations are given in *Tab. 4.6* .

***Tab. 4.6:*** *Fatigue life according to 1-mm stress method*

| | **CAT.** $\Delta\sigma_C$ | **$K_s$** | **$N_{pr}$** ($\Delta\sigma$=Cat.) | **$N_p$** ($\Delta\sigma$=Cat.) | **$N_p$** ($\Delta\sigma$=102MPa) |
|---|---|---|---|---|---|
| Case_20_12_400_S(150)_W(150) | 80 | 1.29 | 4.15E+06 | 1.95.E+06 | 9.39.E+05 |
| Case_20_12_80_S90° | 71 | 1.55 | 5.93E+06 | 1.61.E+06 | 5.42.E+05 |
| Case_20_12_400_S30°_W30° | 71 | 1.70 | 5.93E+06 | 1.21.E+06 | 4.09.E+05 |
| Case_20_12_400_S30° | 71 | 1.77 | 5.93E+06 | 1.07.E+06 | 3.61.E+05 |
| Case_20_12_400_S45° | 71 | 1.87 | 5.93E+06 | 9.11.E+05 | 3.07.E+05 |
| Case_20_12_400_S90° | 56 | 1.94 | 1.21E+07 | 1.65.E+06 | 2.74.E+05 |
| Case_30_12_400_S90° | 56 | 1.98 | 1.21E+07 | 1.55.E+06 | 2.56.E+05 |
| Case_40_12_400_S90° | 56 | 2.03 | 1.21E+07 | 1.44.E+06 | 2.38.E+05 |
| Case_20_20_400_S90° | 56 | 2.04 | 1.21E+07 | 1.43.E+06 | 2.36.E+05 |
| Case_60_12_400_S90° | 56 | 2.09 | 1.21E+07 | 1.32.E+06 | 2.18.E+05 |
| Case_100_12_400_S90° | 56 | 2.15 | 1.21E+07 | 1.21.E+06 | 2.00.E+05 |

Comparing the predicted fatigue lives for *Case_20_20_400_S90°* using the 1-mm stress method (1'430'000 cycles) and by means of LEFM crack propagation (around 2'200'000 cycles), one sees that the result is encouraging. However some adjustments still need to be made (compute the characteristic values for same failure probability rate, define a unique failure criteria, etc.) in order to have a sound comparison basis.

In Tab. 4.7, a comparison between Eurocode 3 categories (identical to SIA263 categories [SIA 263]) and 1mm stress method is made.

***Tab. 4.7:*** *Fatigue strength comparison between Eurocode 3 categories and 1mm stress method results*

| | **CAT.** $\Delta\sigma_C$ | **EC3** $\frac{\Delta\sigma_C^{(Case\_i)}}{\Delta\sigma_C^{(Case\_20\_12\_400\_S90°)}}$ | **1mm method** $\frac{K_s^{(Case\_20\_12\_400\_S90°)}}{K_s^{(Case\_i)}}$ |
|---|---|---|---|
| Case_20_12_400_S(150)_W(150) | 80 | 143% | 151% |
| Case_20_12_80_S90° | 71 | 127% | 126% |
| Case_20_12_400_S30°_W30° | 71 | 127% | 114% |
| Case_20_12_400_S30° | 71 | 127% | 110% |
| Case_20_12_400_S45° | 71 | 127% | 104% |
| Case_20_12_400_S90° | 56 | 100% | 100% |
| Case_30_12_400_S90° | 56 | 100% | 98% |
| Case_40_12_400_S90° | 56 | 100% | 95% |
| Case_20_20_400_S90° | 56 | 100% | 95% |
| Case_60_12_400_S90° | 56 | 100% | 93% |
| Case_100_12_400_S90° | 56 | 100% | 90% |

From Tab. 4.7 and taking *Case_20_12_400_S90°* as a reference for comparison we can see that:

1. *Case_20_12_400_S(150)_W(150)* exhibits relevant fatigue strength increase (151%), compatible with its Eurocode 3 category;
2. *Case_20_12_400_S45°,* although classified as CAT 71 in Eurocode 3 – Part 1-9 [prEN 1993-1-9:2003], doesn't seem to be so gainful (104% of the reference case fatigue strength);
3. The attachment with angle of 30° is more advantageous than the one with 45° (almost no gain in fatigue resistance for the latter);
4. When comparing the welding angles 30° and 45° the increase in fatigue strength seems to be not so significant, around 4% (and difficult to implement in practice);
5. Fatigue strength decreases slightly with main plate thickness and also with attachment (for constant length of 400 mm). The reduction is 10% when increasing the main plate thickness from 20 to 100 mm. This reduction, small compared to other effects, is not included in the current codes.

# 5 CONCLUSIONS

When comparing stress intensity factors, SIF, to stress concentration factors, SCF, and to geometric stress, $K_t$, (Tab. 5.1), it is clear that for the longitudinal stiffeners case, the hot spot stress and the stress intensity factor near the surface are not giving the same information and ranking of the cases.

***Tab. 5.1:*** *Comparison of SCF, SIF and $K_t$(1mm) rankings.*

| | SCF a | SCF b | SIF | $K_t$ (1mm) |
|---|---|---|---|---|
| | Case_100_12_400_S90° | Case_20_12_400_S(150)_W(150) | Case_20_12_400_S(150)_W(150) | Case_20_12_400_S(150)_W(150) |
| | Case_60_12_400_S90° | Case_20_20_400_S90° | Case_20_12_400_S30° | Case_20_12_80_S90° |
| | Case_30_12_400_S90° | Case_20_12_400_S30° | Case_20_12_80_S90° | Case_20_12_400_S30°_W30° |
| | Case_40_12_400_S90° | Case_20_12_400_S30°_W30° | Case_20_12_400_S30°_W30° | Case_20_12_400_S30° |
| | Case_20_12_80_S90° | Case_20_12_80_S90° | Case_40_12_400_S90° | Case_20_12_400_S45° |
| | Case_20_12_400_S(150)_W(150) | Case_30_12_400_S90° | Case_20_12_400_S90° | Case_20_12_400_S90° |
| | Case_20_12_400_S30° | Case_20_12_400_S90° | Case_20_12_400_S45° | Case_30_12_400_S90° |
| | Case_20_20_400_S90° | Case_20_12_400_S45° | Case_30_12_400_S90° | Case_40_12_400_S90° |
| | Case_20_12_400_S90° | Case_40_12_400_S90° | Case_20_20_400_S90° | Case_20_20_400_S90° |
| | Case_20_12_400_S30°_W30° | Case_100_12_400_S90° | Case_60_12_400_S90° | Case_60_12_400_S90° |
| | Case_20_12_400_S45° | Case_60_12_400_S90° | Case_100_12_400_S90° | Case_100_12_400_S90° |

Although for hollow section details, the hot-spot stress has revealed to be effective to characterise fatigue resistance, this link is not obvious for longitudinal attachments details. More parameters should be put in consideration, because fatigue life depends not only on the surface geometric stress but also on the stress distribution in the depth along the anticipated crack path. This is the basis for the 1 mm stress method proposed by Xiao and Yamada.

If the *SCF* values obtained for the different cases are compared with respective fatigue details categories, *type b* seems to be more closely linked to fatigue resistance, which suggests that the effect of the weld profile might play a significant role. On the contrary, *type a SCF*s do not seem appropriate to evaluate the fatigue behaviour of longitudinal attachment details.

Stress intensity factor values, SIF, relate quite well to fatigue categories of the details when looking at a 0.15mm crack depth, but not so well when looking at SIF values for deeper cracks. This leads to questions about current Eurocode 3 or SIA263 [SIA 263] category classification. A fatigue life study based upon BEASY crack growth simulations for the different cases could bring new elements into the discussion. Furthermore, information about details on SBB bridges, for example on weld angle, weld size, range of thicknesses of the plates would help in reorganising the details in different classes and separating the thickness effect from experimental error.

The 1mm stress method $K_t$ (or $K_s$) values relate very well to fatigue categories of the details. When compared to the surface extrapolation technique for hot-spot stress determination, the 1mm stress method has the

advantage that it is able to account for the thickness effect observed in welded joints. Thus we think it is currently the most adequate to categorize new details on SCF basis.

According to the results obtained with the 1mm the following conclusions can be stated:

1. **Round attachment with round weld** details (R ≈ 150 mm) exhibit the best fatigue strength;
2. Fatigue strength of **45° attachments is similar to 90° attachments**;
3. The **attachment with 30° is more advantageous than the one with 45°**;
4. When comparing the **welding angles 30° and 45°** the **increase in fatigue strength seems to be not so significant, around 4%** (and difficult to implement in practice);
5. **Fatigue strength decreases slightly with main plate thickness and also with attachment thickness** (for constant length of 400 mm). The reduction is 10% when increasing the main plate thickness from 20 to 100 mm. This reduction, small compared to attachment length, is not included in the current codes.

## ACKNOWLEDGEMENTS

The authors would like to thank Prof. K. Yamada (Nagoya University Chikusa-ku, Nagoya, Japan) for the interesting discussions and support concerning the 1-mm stress method. The authors are also grateful for the contributions of Dr. S. Herion (University of Karlsruhe, Germany) for discussions on hot spot stress method, S. Höhler (RWTH Aachen, Germany) for introduction to Beasy and Dr. S. Haldimann (ICOM / SBB) for the valuable comments and critical review of document.

# 6 REFERENCES


[BEASY 2003] ***BEASY User Guide***, Computational mechanics BEASY Ltd, Ashurst, Southhampton, UK, 2003.

[Castiglioni 1989] CASTIGLIONI, C., ***Influences of some geometrical parameters on stress concentration in longitudinal welded attachments***, Construzioni metalliche, No. 41, pp. 1-21, 1989.

[Castiglioni et al. 1992] CASTIGLIONI, C. A., GIANOLA, P., ***Parametric analysis of weld toe stress concentration in longitudinal attachments***, Welding International, 1992.

[Hirt TGC 10] HIRT, M.A., BEZ, R., ***Construction Métallique***, Traité de Génie Civil volume 10, Presses polytechniques universitaires romandes (PPUR), Lausanne, Suisse, 1996.

[Hobbacher 1993] HOBBACHER, A., ***Stress intensity factors of welded joints***, Engineering Fracture Mechanics, pp. 173-182, Pergamon, 1993.

[Hobbacher 2003] HOBBACHER, A., ***Recommendations for fatigue design of welded joints and components****, IIW document XIII-1965-03 / XV-1127-03*, International Institute of welding, July 2003.

[Newman et al. 1984] NEWMAN, J. C. , RAJU, I. S., ***Stress-intensity factor equations for cracks in three dimensional finite bodies subjected to tension and bending loads***, Technical Memorandum, No. 85793, NASA, USA, 1984.

[Niemi 2000] NIEMI, E., ***Structural Stress Approach to Fatigue Analysis of Welded Components***, International Institute of Welding (IIW), Doc. XIII-1819-00, pp. 1-44, IIW, 2000.

[Poutiainen et al. 2004.1] POUTIAINEN, I., TANSKANEN, P. , MARQUIS, G., ***Finite element methods for structural hot spot stress determination—a comparison of procedures***, International Journal of Fatigue, Vol. 26, pp. 1147–1157, Elsevier, 2004.

[prEN 1993-1-9:2003] *Eurocode 3:* ***Design of steel structure – Part 1.9: Fatigue strength of steel structures***, prEN 1993-1-9:2003, CEN, November 2003.

[Radaj 1995] RADAJ, D., ***Ermüdungsfestigkeit,*** Springer-Verlag, 1995.

[SIA 263] ***SIA 263: Stahlbau***, Schweizerischer Ingenieur- und Architektenverein, Zürich, 2003.

[Xiao et al. 2004] XIAO, Z.-G., YAMADA, K., ***A method of determining geometric stress for fatigue strength evaluation of steel welded joints***, International Journal of Fatigue 26 (2004) 1277–1293, Vol. 26, Elsevier, 2004.

[Zettlemoyer 1976] ZETTLEMOYER, N., ***Stress Concentration and Fatigue of Welded Details***, Lehigh University, USA, October 1976.

# 7 ANNEXES

## 7.1 SHORT BIBLIOGRAPHY ON LONGITUDINAL ATTACHMENTS SOLUTIONS

Title: **STRESS INTENSITY FACTORS OF WELDED-JOINTS (VOL 46, PG 181, 1993)**
Author(s): **HOBBACHER A**
Source: ENGINEERING FRACTURE MECHANICS 49 (2): 323-323 SEP 1994
Document Type: Correction, Addition
Language: English
Publisher: PERGAMON-ELSEVIER SCIENCE LTD, THE BOULEVARD, LANGFORD LANE, KIDLINGTON, OXFORD, ENGLAND OX5 1GB
IDS Number: PW233
ISSN: 0013-7944

Title: **STRESS INTENSITY FACTORS OF PLATES UNDER TENSILE LOAD WITH WELDED-ON FLAT SIDE GUSSETS**
Author(s): **HOBBACHER A**
Source: ENGINEERING FRACTURE MECHANICS 41 (6): 897-905 APR 1992
Document Type: Article
Language: English
Abstract: The effects of stress concentrations on stress intensity factors at plates under tensile load with welded-on flat side gussets have been studied. The correction function Yu of the crack configuration has been split into a function for the general configuration Y and a function for the local stress concentration Mk due to the weld and the gusset. The Mk values have been calculated by finite element analysis and by a simplified procedure based on the weight function approach. The results have been interpolated, giving a parametric formula for a wide range of variation in dimensions.
Addresses: HOBBACHER A (reprint author), FACHHSCH WILHELMSHAVEN, WELDING LAB, WILHELMSHAVEN, W-2940 GERMANY
Publisher: PERGAMON-ELSEVIER SCIENCE LTD, THE BOULEVARD, LANGFORD LANE, KIDLINGTON, OXFORD, ENGLAND OX5 1GB
IDS Number: HR722
ISSN: 0013-7944

Title: **A BRIEF NOTE ON THE ESTIMATION OF STRESS-CONCENTRATION FACTORS OF SHARP EDGE NOTCHES**
Author(s): SCHIJVE J
Source: INTERNATIONAL JOURNAL OF FATIGUE 8 (2): 95-97 APR 1986
Document Type: Note
Language: English
Addresses: SCHIJVE J (reprint author), DELFT UNIV TECHNOL, DEPT AEROSP ENGN, POB 5058, DELFT, 2600 GB NETHERLANDS
Publisher: BUTTERWORTH-HEINEMANN LTD, THE BOULEVARD, LANGFORD LANE, KIDLINGTON, OXFORD, OXON, ENGLAND OX5 1GB
IDS Number: A9093
ISSN: 0142-1123

Title: **A STRUCTURAL STRESS DEFINITION AND NUMERICAL IMPLEMENTATION FOR FATIGUE ANALYSIS OF WELDED JOINTS**
Author(s): Dong P
Source: INTERNATIONAL JOURNAL OF FATIGUE 23 (10): 865-876 NOV 2001
Document Type: Article

Language: English
Abstract: A mesh-size insensitive structural stress definition is presented in this paper. The structural stress definition is consistent with elementary structural mechanics theory and provides an effective measure of a stress state that pertains to fatigue behavior of welded joints in the form of both membrane and bending components. Numerical procedures for both solid models and shell or plate element models are presented to demonstrate the mesh-size insensitivity in extracting the structural stress parameter. Conventional finite element models can be directly used with the structural stress calculation as a post-processing procedure. To further illustrate the effectiveness of the present structural stress procedures, a collection of existing weld S-N data for various joint types were processed using the current structural stress procedures. The results strongly suggests that weld classification based S-N curves can be significantly reduced into possibly a single master S-N curve, in which the slope of the S-N curve is determined by the relative composition of the membrane and bending components of the structural stress parameter. The effects of membrane and bending on S-N behaviors can be addressed by introducing an equivalent stress intensity factor based parameter using the structural stress components. Among other things, the two major implications are: (a) structural stresses pertaining to weld fatigue behavior can be consistently calculated in a mesh-insensitive manner regardless of types of finite element models; (b) transferability of weld S-N test data, regardless of welded joint types and loading modes, can be established using the structural stress based parameters. (C) 2001 Elsevier Science Ltd. All rights reserved.
Author Keywords: structural stress; finite element analysis; welded joints; fatigue; notch stress; stress concentration; mesh-size sensitivity
Addresses: Dong P (reprint author), Battelle Mem Inst, Ctr Welded Struct Res, Columbus, OH 43016 USA
Battelle Mem Inst, Ctr Welded Struct Res, Columbus, OH 43016 USA
Publisher: ELSEVIER SCI LTD, THE BOULEVARD, LANGFORD LANE, KIDLINGTON, OXFORD OX5 1GB, OXON, ENGLAND
IDS Number: 484JW
ISSN: 0142-1123

Title: **IMPROVING THE FATIGUE PERFORMANCE OF FILLET WELD TERMINATIONS**
Author(s): Dimitrakis SD, Lawrence FV
Source: FATIGUE & FRACTURE OF ENGINEERING MATERIALS & STRUCTURES 24 (6): 429-438 JUN 2001
Document Type: Article
Language: English
Abstract: A specialty designed stress-concentration-reducing part was incorporated in the wraparound welds at the ends of fillet-welded longitudinal attachments, that is, at fillet weld terminations-ubiquitous weld details having a notoriously poor fatigue resistance. The incorporation of this part at the terminations of the fillet-welds substantially decreased the weld toe stresses in those locations where fatigue cracks customarily start, reduced weld toe residual stresses and promoted increases in the weld-toe notch-root radius. In the long-life regime, the incorporation of these small, added parts increased weldment fatigue life by 300% and fatigue strength by 30%. It was found that the full benefit of the added part could only be achieved when welding processes were employed that avoided the production of cold-lap weld-toe defects.
Author Keywords: fatigue of weldments; fatigue life improvement; mechanical properties of weldments; welding; fatigue
Addresses: Lawrence FV (reprint author), Univ Illinois, Dept Civil Engn, Room 1110 MC-250, Urbana, IL 61801 USA
Univ Illinois, Dept Civil Engn, Urbana, IL 61801 USA
Publisher: BLACKWELL SCIENCE LTD, P O BOX 88, OSNEY MEAD, OXFORD OX2 0NE, OXON, ENGLAND
IDS Number: 469CM
ISSN: 8756-758X

Title: **Fatigue strength of intersecting attachments**
Author(s): Xiao ZG, Yamada K
Source: JOURNAL OF STRUCTURAL ENGINEERING-ASCE 131 (6): 924-932 JUN 2005
Document Type: Article
Language: English
Abstract: Experimental investigations are carried out on intersecting attachments to investigate their fatigue strengths. Two types of intersecting attachments are studied, i.e., the T type with one longitudinal attachment intersecting a transverse stiffener at one end, and the H type with a longitudinal attachment intersecting two transverse stiffeners at both ends. The length of the longitudinal attachment in the T type is changed to study its effects on fatigue strength. The scalloped version of the specimens, free of welds at the intersection of the transverse and longitudinal attachments, is also investigated. Test results show that the fatigue strength of the T type attachment is comparable to that of the single longitudinal attachment. The fatigue strength of the H type attachment is in between those of the single longitudinal and transverse attachments. The introduction of the scallops does not influence fatigue strength significantly, but results in a change in the locations of fatigue cracks in the H type attachments. The method suggested by the writers for fatigue strength evaluation of weld toe failures is demonstrated as suitable for evaluating fatigue strength of intersecting attachments.
KeyWords Plus: WELDED-JOINTS; STRESS; STEEL
Addresses: Xiao ZG (reprint author), Nagoya Univ, Dept Civil Engn, Chikusa Ku, Furo Cho, Nagoya, Aichi Japan
Nagoya Univ, Dept Civil Engn, Chikusa Ku, Nagoya, Aichi Japan
Nagoya Univ, Grad Sch Environm Studies, Dept Environm Engn & Architecture, Chikusa Ku, Nagoya, Aichi 4648603 Japan
Publisher: ASCE-AMER SOC CIVIL ENGINEERS, 1801 ALEXANDER BELL DR, RESTON, VA 20191-4400 USA
IDS Number: 927VK
ISSN: 0733-9445

Title: **A METHOD OF DETERMINING GEOMETRIC STRESS FOR FATIGUE STRENGTH EVALUATION OF STEEL WELDED JOINTS**
Author(s): Xiao ZG, Yamada K
Source: INTERNATIONAL JOURNAL OF FATIGUE 26 (12): 1277-1293 DEC 2004
Document Type: Article
Language: English
Abstract: This paper presents a new method for evaluating the geometric or structural stress in welded constructions. The method is based on the computed stress value 1-mm below the surface in the direction corresponding to the expected crack path. The total stress distribution along the crack path direction is considered to be the sum of the geometric stress caused by the structural geometry change and the non-linear local stress produced by the weld itself. Linear elastic fracture mechanics is used to correlate the total stress based crack propagation life and the local stress based crack propagation life to explain the geometric stress evaluated 1-mm below the surface. Validity of the method is further verified by analyzing fatigue test results for several typical welded joints reported in literature. When compared to the surface extrapolation technique for structural hot spot stress evaluation, the proposed method has the additional advantage in that it is able to account for the size and thickness effect observed in welded joints. 
Author Keywords: fatigue; welded joint; geometric stress; hot spot stress; finite element method
Addresses: Xiao ZG (reprint author), Nagoya Univ, Dept Civil Engn, Chikusa Ku, Nagoya, Aichi 4648603 Japan Nagoya Univ, Dept Civil Engn, Chikusa Ku, Nagoya, Aichi 4648603 Japan
Nagoya Univ, Grad Sch Environm Studies, Dept Environm Engn & Architecture, Chikusa Ku, Nagoya, Aichi 4648603 Japan
Publisher: ELSEVIER SCI LTD, THE BOULEVARD, LANGFORD LANE, KIDLINGTON, OXFORD OX5 1GB, OXON, ENGLAND
IDS Number: 866AI
ISSN: 0142-1123

## 7.2 HOT-SPOT STRESSES CALCULATION

| Case | CAT | SCF | | | Model | Longitudinal Stress |
|---|---|---|---|---|---|---|
| | | a | | b | | |
| | | lin | quad | quad | | |
| Case_20_12_80_S90° | 71 | 1.22 | 1.26 | 1.74 | 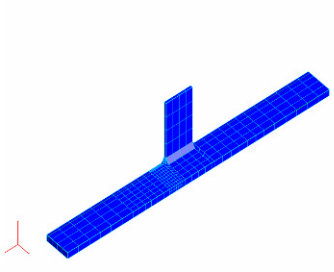 | 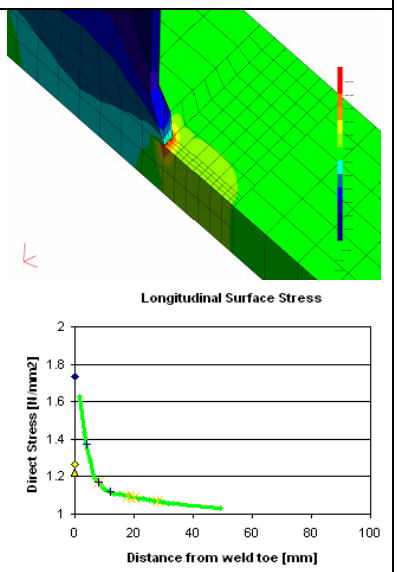  |
| Case_20_20_400_S90° | 56 | 1.33 | 1.33 | 1.49 | 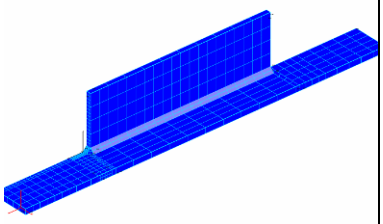 | 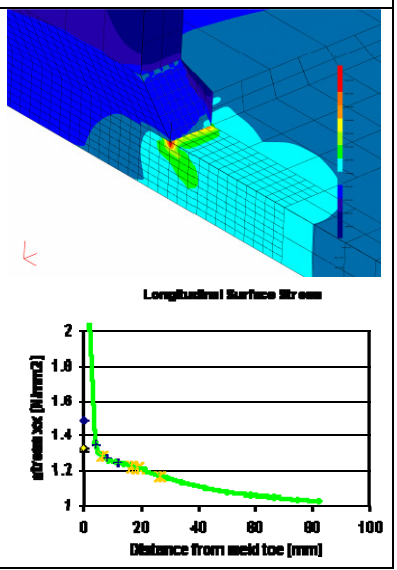  |

| | | | | | | |
|---|---|---|---|---|---|---|
| Case_20_12_400_S90° | 56 | 1.31 | 1.33 | 1.92 | 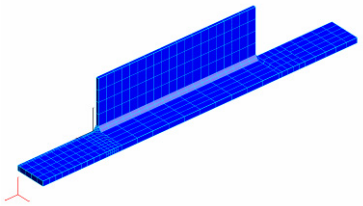 | 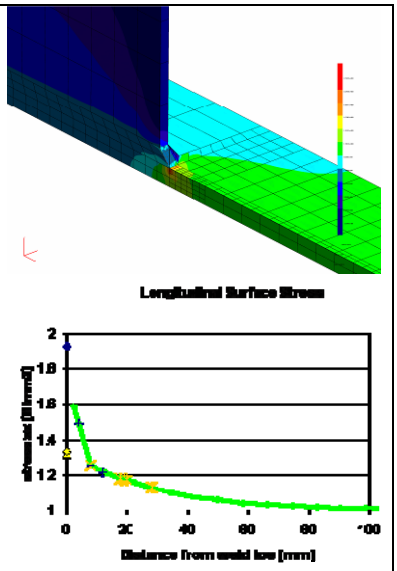  |
| Case_40_12_400_S90° | 56 | 1.19 | 1.24 | 2.10 | 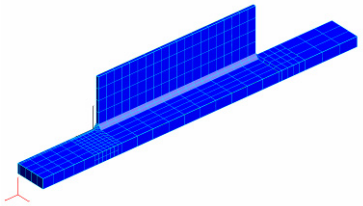 | 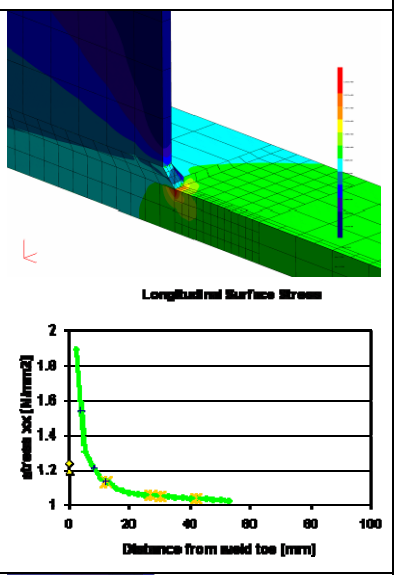  |
| Case_30_12_400_S90° | 56 | 1.08 | 1.17 | 1.88 | 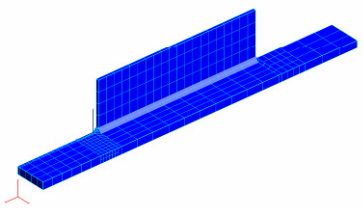 | 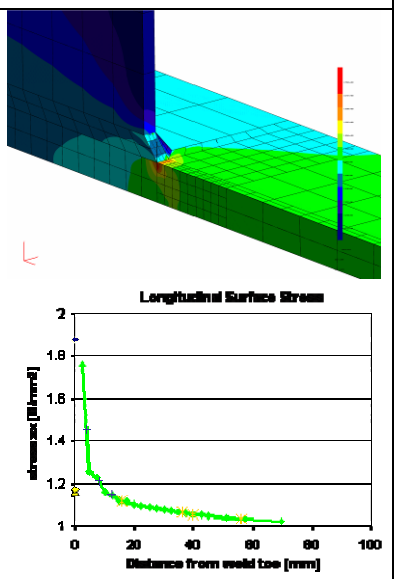  |

| | | | | | | |
|---|---|---|---|---|---|---|
| Case_60_12_400_S90° | 56 | 1.08 | 1.10 | 2.61 | 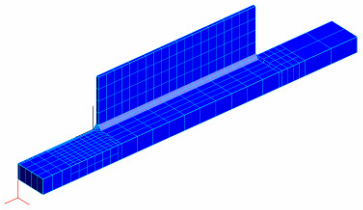 | 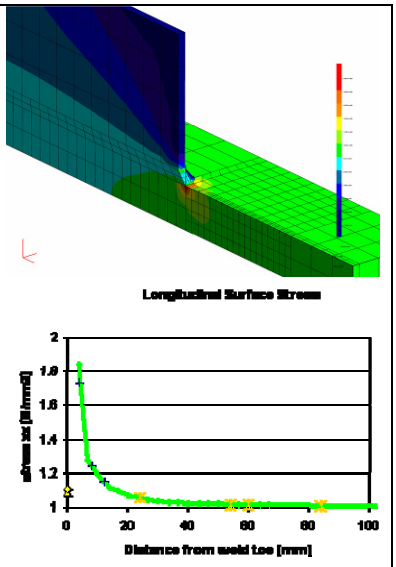  |
| Case_100_12_400_S90° | 56 | 1.03 | 1.04 | 2.51 | 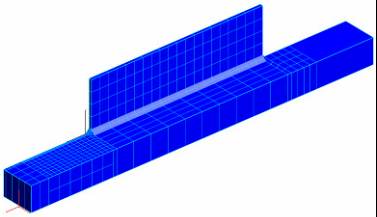 | 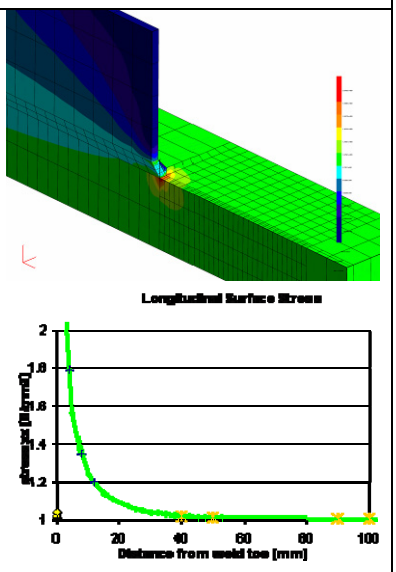  |
| Case_20_12_400_S45° | 71 | 1.34 | 1.37 | 2.00 | 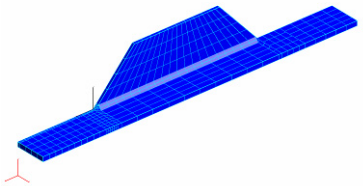 | 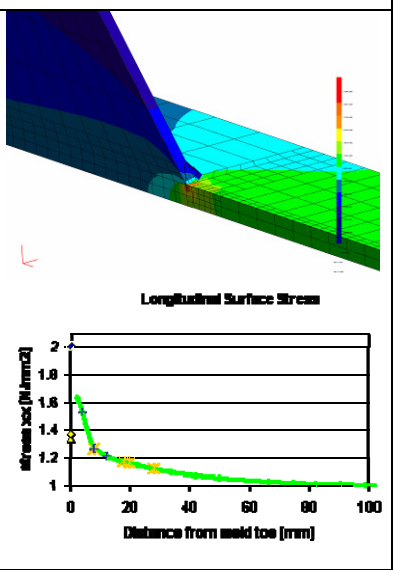  |

| | | | | | | |
|---|---|---|---|---|---|---|
| Case_20_12_400_S30°_W30° | 71 | 1.33 | 1.36 | 1.71 | 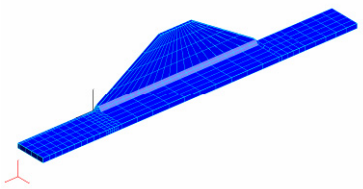 | 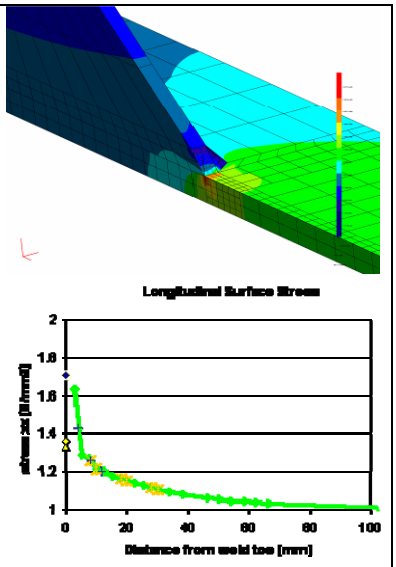  |
| Case_20_12_400_S30° | 71 | 1.29 | 1.33 | 1.55 | 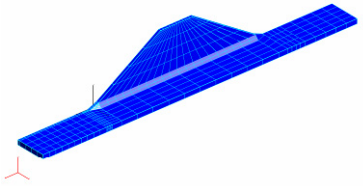 | 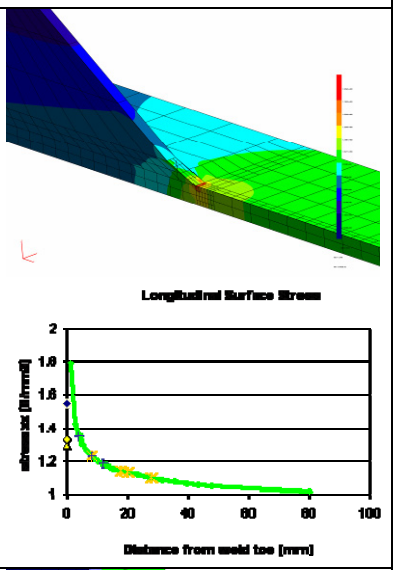  |
| Case_20_12_400_S(150)_W(150) | 80 | 1.27 | 1.30 | 1.41 | 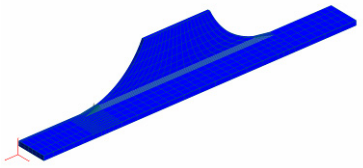 | 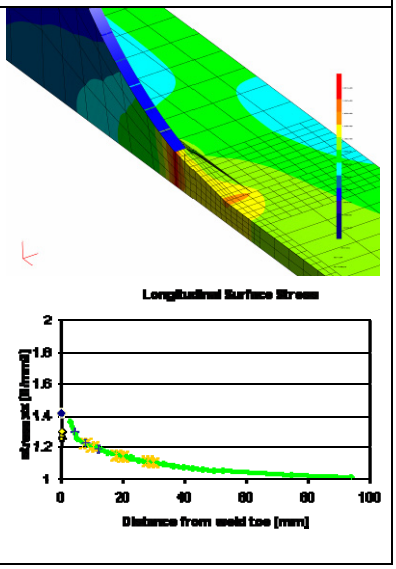  |